IEEJ TRANSACTIONS ON ELECTRICAL AND ELECTRONIC ENGINEERING
IEEJ Trans 2019; **14**: 1532–1542
Published online in Wiley Online Library (wileyonlinelibrary.com). DOI:10.1002/tee.22973

Paper

A Novel Locomotive Auxiliary Converter Control Strategy with Harmonic Suppression for Avoiding Resonance Voltage Accidents in an Electrified Railway

Meijun Mu, Non-member
Zhongping Yang, Non-member
Fei Lin, Non-member
Shihui Liu, Non-member

In recent years, the AC-DC-AC electric locomotives have been wildly applied in electrified railways, deteriorating the current quality of network. Therefore, filters in electrified railways are essential. However, considering the volume and weight of filters, it is inappropriate to install them on locomotives. And resonance accident caused by high-frequency harmonics is hard to suppress because of the low switching speed of high-power Si-based devices. In this article, a novel locomotive auxiliary converter control strategy with harmonic suppression function is proposed to filter harmonic currents injected into the traction supply network. By controlling the auxiliary converter, the strategy could complete the function of rectification and filtering, converting power for auxiliary equipment, filtering the harmonic current, and suppressing resonance accidents with the high-frequency characteristics of *SiC* devices. For compensating high-frequency harmonics, the parameters of main circuit and control scheme are analyzed to ensure a stable system. The feasibility of the scheme is verified by simulation and RT-LAB hardware-in-loop experiment. © 2019 Institute of Electrical Engineers of Japan. Published by John Wiley & Sons, Inc.

Keywords: electrified railway; electric locomotive; resonance suppression; power quality

Received 1 June 2018; Revised 29 March 2019

1. Introduction

With the development of electrified railways, AC-DC-AC electric locomotives have been widely used, so multiple frequency harmonic current would be injected into public supply networks during the operation of electric locomotives, deteriorating the power quality and causing overvoltage protection [1]. In addition, resonance accidents might happen, which means the voltage of traction network would rise significantly, leading to breakdown of equipment along the network. In Zürich, Switzerland, locomotives were automatically shut down by protective equipment because of high harmonic current. In 2017, the HX_D2 electric locomotive caused a resonance accident at Datong substation in China, leading to the tripping operation of the locomotive. The accident frequency is 1750 Hz [2]. The frequency of harmonic current focuses on 150 Hz, 250 Hz, 350 Hz etc., as well as the high-order frequency around integral multiple of the switching frequency.

As for measures to suppress the harmonics, first of all, we can reconstruct traction substation, such as installing passive or active filters. The passive filter methods like installing a inductance and capacity filter or a high pass filter at traction substation can filter specific harmonics, but are unable to compensate the harmonic current dynamically when frequency changes [3,4]. Based on power electronic technology, we can also install active power filter equipment along with a step-down transformer to realize the dynamic compensation of harmonic current [5,6], such as the method of using two 'back to back' single-phase full bridge converters and a power quality compensation system composed of a three-phase voltage source converter and a thyristor switching capacitor. For the methods mentioned above, high-power switching devices and step-down transformers are required, leading to the complexity of the system and large capacity of the active part, which are difficult to be applied in project [7,8].

For compensation methods on electric locomotives, similar to mentioned above, passive filters like a inductance, capacity and inductance filter is inappropriate when parameters change [9]. Active filters increase the weight of locomotives, which is not conducive for lightweight rail transit [10]. The method of eliminating the resonant frequency point by modifying the switching frequency of traction converters could avoid resonance at some certain frequency, unable to eliminate all the resonance frequency as well as the 150 Hz, 250 Hz etc. harmonic currents.

In this article, a novel locomotive auxiliary converter control strategy is proposed, which means we can control the auxiliary converter to improve the power quality of the network without installing extra devices. At the same time, the auxiliary converter could convert power for auxiliary equipment such as lights and air conditioners on electric locomotives. In this strategy, a direct current (DC) voltage controller and a fundamental current controller are applied to complete the rectification function, the harmonic current controller is applied to track and compensate the harmonic current of the grid side until the harmonic current is filtered, thereby improving the power quality of the electrified railway and suppressing resonance voltage. The scheme use *SiC* devices to produce compensation current whose frequency is high and around the integer times of switching frequency of traction converters. Meanwhile, the application of *SiC* devices could reduce the loss and weight of converters.

The scheme use *SiC* devices for the auxiliary converter to produce compensation current whose frequency is a few integer times higher than the switching frequency of traction converters.

[a] Correspondence to: Zhongping Yang. E-mail: zhpyang@bjtu.edu.cn

College of Electrical Engineering, Beijing Jiaotong University, Shangyuan No. 3, Haidian District Beijing, China

Meanwhile, the application of *SiC* devices also reduces the loss and weight of the auxiliary converters.

However, if full *SiC* devices are applied in traction converters, the switching frequency could be increased significantly and hence both resonance frequencies could be avoided and power quality in the electric traction network could be improved. This advanced method has been applied in N700s in Japan [11]. Because the high-power full *SiC* technology has not been easily available, the strategy proposed in this article is mainly aimed at reforming the existing locomotives with Si-based traction inverters to solve the resonance problems. The auxiliary converters on these locomotives operate at lower power and hence *SiC* technology could be easily adopted for them.

The tracking control method of harmonic current loop in this scheme plays an important part in compensating harmonics. Proportional integral (PI) control is hard to track AC reference current with no error [12]. The control method based on the synchronous reference frame has to invent a q-axis component, which is complicated in a single-phase bridge circuit [13,14]. The proportional resonance (PR) controller could track the sinusoidal signal with no error by producing an infinite gain at the resonance frequency, but parameter tuning and digitization are complex to obtain a stable and optimized system [15–17]. For the purpose of compensating multiple-frequency harmonic currents generated during the operation of electric locomotives, multiple PR controllers are applied to track the harmonic current commands without error in this article.

To apply the proposed control scheme to practice, we need to digitalize it and tuning the parameters of the controller. Tustin with prewarping method would keep frequency from shifting at the resonance frequency point, and the phase delay of the system at this point is tiny after discretization, ensuring a larger gain at the resonance point [18]. In references [19–22], parameters of multiple parallel resonant controller are designed, respectively, to satisfy the stability of the system, but the parameter design was not mentioned at high frequency.

For high-frequency harmonic controllers, the digital delay link causes phase lags in current loop during discretization. With the increase of the harmonic frequency, the phase frequency characteristics will probably pass through 180°, leading to instability of the current loop. Also, when the resonant frequency approaches to the Nyquist frequency, the system tends to be unstable.

In view of the above problems in digital implementation, this article adopts the Tustin with prewarping method to discretize the control scheme, and design the critical parameters of the controller in the discrete domain, so as to maintain the stability of the system and get a superior control effect. The stability issue is analyzed, and feedback control is introduced to solve the problem of phase lag caused by digital delay.

This article is organized as follows. Section 2 introduces the causes and effects of the harmonic generation of electrified railways. Section 3 explains the control principle of a multifunction converter, and the analysis of the main circuit. Section 4 presents the control scheme of the converter and its digital implementation, including its parameter and stability analysis. Section 5 verifies the control scheme by simulation and hardware-in-the-loop experiment. Section 6 is conclusion.

2. Causes and Effects of Harmonics in Electrified Railways

Figure 1 shows the main circuit of the AC-DC-AC electric locomotive. T represents traction connect network and R is the rail. The single-phase alternating current provided by traction substation flows to the traction drive system and auxiliary power unit through the main transformer, drives the locomotive, and provides power for the locomotive auxiliary equipment. At the same time, the electric locomotive, as a nonlinear load, injects some specific harmonics into the traction network. The main harmonic source is the single-phase four quadrant converter (4QC) of the traction side.

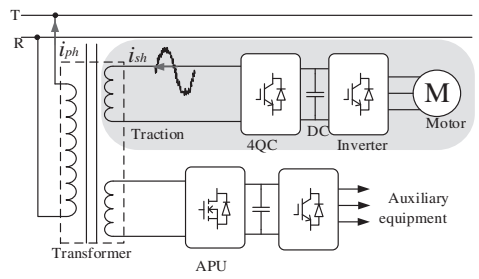

Fig. 1. Main circuit of electric locomotive connected into the traction network

2.1. Causes of harmonics The DC-side output voltage of the single-phase 4QC contains the second harmonic component, which introduces the 3rd harmonic component to the reference current through the DC voltage control loop, thus generating the 3rd harmonic on the AC side. The 3rd harmonic generates 4th harmonic component on the DC side, leading to the 5th AC side harmonic. In this way, the low harmonic of 3rd, 5th, 7th, and 9th harmonic current will flow into the traction network during the operation of locomotive.

Due to the application of pulse width modulation (PWM) modulation technology, the expression of harmonic current injected into the traction network of the traction side single-phase 4QC is shown as follows [23]:

$$i_{Nn}(t) = \sum_{m=2,4\ldots}^{\infty} \sum_{n=\pm1,\pm3\ldots}^{\infty} \frac{4U_{d2}}{m\pi L_2(m\omega_c+n\omega_1)} J_n\left(\frac{m\pi M}{2}\right) \cos\frac{m\pi}{2} \sin\frac{n\pi}{2} \sin(m\omega_c t + n\omega_1 t + m\alpha + n\beta) \tag{1}$$

In this formula, U_{d2} is the DC voltage, L_2 is the inductance at the AC side, ω_c is the switching angle frequency, ω_1 is the fundamental angle frequency, M is the modulation, α is the carrier initial angle, and β the initial phase angle of the modulated wave. J_n is the Bessel function.

The harmonic component frequencies of the input current concentrate on the high frequency round the even times of the switching frequency. The larger the value of m in the formula, the smaller the harmonic amplitude. The harmonic content is affected by the modulation, the magnitude of the DC voltage, the effective value of the grid voltage, the net voltage frequency, and the PWM modulation carrier frequency. The amplitude of harmonic is also related to the inductance value of the AC side.

2.2. Effects of harmonics As the main harmonic source of electrified railways, electric locomotives generate a great deal of power harmonics during operation, and the harmonics flow into the power grid through the traction power supply system, leading to distortion of the voltage waveform. Figure 2 shows the effects of harmonics.

1. Harmonics not only affect the life of electrical equipment in the power grid, but also shorten the life of the equipment of the electrified railway. They would cause obvious interference to the adjacent communication system, cause misoperation of protective relays, and bring about greater errors in electrical measurement instruments and energy metering.
2. During the operation of the locomotive, the harmonic current generated by the traction converter would be

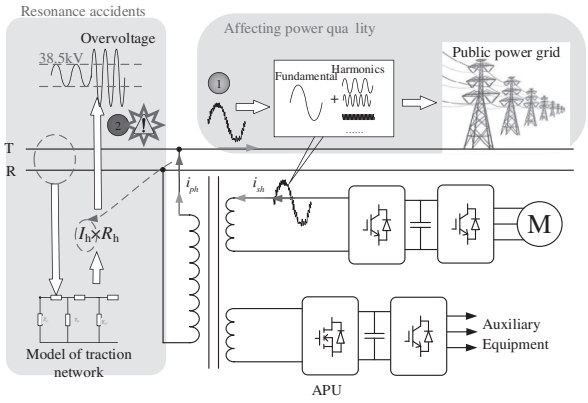

Fig. 2. Effects of harmonics

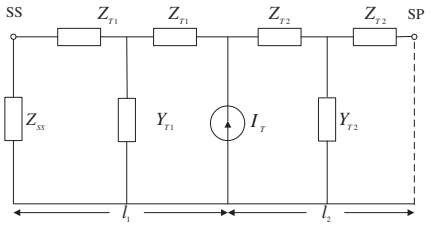

Fig. 3. Traction network T type equivalent circuit

injected into the traction network, which forms a resonance circuit with the impedance of the traction network, causing the train terminal voltage to rise obviously.

To analyze the characteristics of the traction network, we usually build a T-type equivalent circuit model [24].

The train is equivalent to a current source I_T. Z_{ss}, Z_{Tn}, and Y_{Tn} are equivalent parameters of the traction substation and line (Fig. 3).

Let Z_1 and Z_2 be the impedance from the locomotive position to the traction substation and the direction of the partition, respectively.

$$Z_1 = Z_c \frac{Z_{ss}\cosh(\gamma L_1) + Z_c \sinh(\gamma L_1)}{Z_{ss}\sinh(\gamma L_1) + Z_c \cosh(\gamma L_1)}$$
$$Z_2 = Z_c \frac{\cosh(\gamma L_2)}{\sinh(\gamma L_2)} \tag{2}$$

γ and Z_c are the propagation constant and characteristic impedance, respectively:

$$\gamma = \sqrt{Z_0 Y_0} \tag{3}$$

$$Z_c = \sqrt{\frac{Z_0}{Y_0}} \tag{4}$$

Z_0,Y_0 are unit length impedance and admittance parameters. The impedance of the location of the train is shown in formula (5).

$$Z_q = \frac{Z_1 Z_2}{Z_1 + Z_2} = \frac{\frac{Z_0}{Y_0}\cosh(\sqrt{Z_0 Y_0} l_2)(Z_{ss}\cosh(\sqrt{Z_0 Y_0} l_1) + Z_c \sinh(\sqrt{Z_0 Y_0} l_1))}{Z_{ss}\sinh(\sqrt{Z_0 Y_0} l) + \frac{Z_0}{Y_0}\cosh(\sqrt{Z_0 Y_0} l)} \tag{5}$$

When the resonance happens,

$$Z_{ss}\sinh(\sqrt{Z_0 Y_0} l) + \frac{Z_0}{Y_0}\cosh(\sqrt{Z_0 Y_0} l) = 0 \tag{6}$$

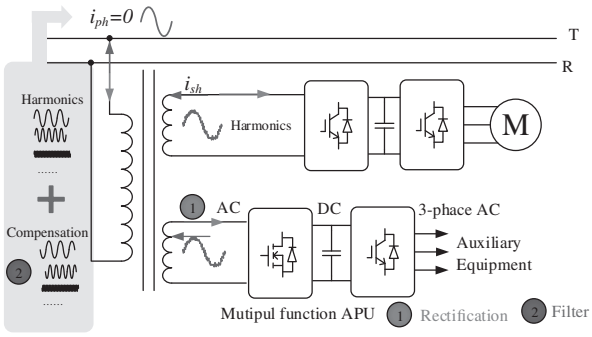

Fig. 4. Introduction of auxiliary converter function

Therefore, Z_q approaches to ∞. The resonance frequency is:

$$f_h = \frac{1}{2\pi\sqrt{L_{ss} C}} \tag{7}$$

If the frequency of the harmonic current injected by the traction converter is equal to this resonance frequency, locomotive terminal voltage amplitude approaches to ∞ .

$$u(j\omega_h) = Z_q \cdot i_T(j\omega_h) \tag{8}$$

The harmonic current injected into the traction network will cause the voltage rise at a specific frequency, resulting in the resonance accident. Therefore, we consider to suppress the resonance by filtering the harmonic current.

3. Control Principle of Multifunction Converter

To filter the harmonic current injected into the traction network by electric locomotive, a novel converter control strategy is proposed in this article, as shown in Fig. 4.

Considering the low power of the auxiliary converter, we apply *SiC* power devices to the auxiliary converter, and achieve the function of rectification and filtering by changing the control algorithm of the auxiliary converter simultaneously.

Figure 4 shows the two functions of the auxiliary converter.

1. For the single-phase rectification function, the single-phase alternating current from the traction power supply network is converted to direct current through 4QC, and then converted to three-phase alternating current for the auxiliary equipment on the locomotive by the inverter.
2. The filtering function is realized by detecting the primary side current of the transformer and controlling the auxiliary converter to produce the compensation current that is inverse to the harmonic current, so that the harmonic current in the traction network is filtered, improving power quality of the power grid, and avoiding the occurrence of resonance accident.

3.1. Analysis of the control principle

The equivalent model of the locomotive main circuit is shown in Fig. 5. n_1, n_2, and n_3 are ratios of the transformer, corresponding to the primary winding, traction winding, and auxiliary winding, respectively. v_p, i_p, v_s, i_s, and v_c, i_c are the voltages and currents of the original side, the traction side, the auxiliary side of the transformer, respectively, in Fig. 5, the value is converted to the auxiliary side. x,r is the equivalent impedance, and u_{ab} is the pulse voltage.

In Fig. 6, V_c, I_c is the voltage and current in the AC side of the auxiliary converter, U_{ab} is the pulse voltage. $j\omega L_3 I_c$ is the voltage of the inductor. C is the capacitor of the DC side. R is the equivalent impedance. U_d is the DC voltage. It shows the voltage and current vector diagrams on the AC side and the equivalent

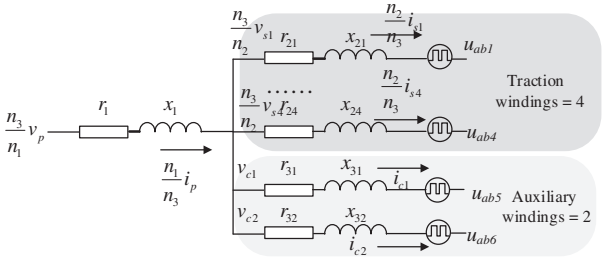

Fig. 5. Electric locomotive equivalent circuit

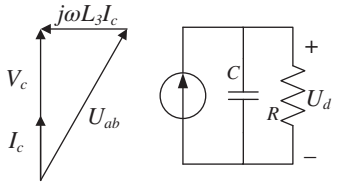

Fig. 6. Equivalent circuit diagram of rectification function

circuit diagram on the DC side when the converter operates at rectification mode. At this time, the pulse rectifier guarantees the sinusoidal output of the AC side by pulse width modulation, and the stable voltage output in the DC side.

The formula (9) indicates the current relationship of the transformer winding in Fig. 5, and the formula (10) is obtained after simplification. Therefore, the harmonic current expression is (11). By controlling the auxiliary current transformer to generate the compensation current i_{ch}, the primary side harmonic current i_{ph} can be reduced to zero, so as to improve the power quality and suppress the resonance.

$$\frac{n_1}{n_3} i_p = \frac{n_2}{n_3} \sum_{n=1}^{4} i_{sn} + \sum_{n=1}^{2} i_{cn} \tag{9}$$

$$n_1 i_p = n_2 i_s + n_3 i_c \tag{10}$$

$$n_1 i_{ph} = n_2 i_{sh} + n_3 i_{ch} \tag{11}$$

3.2. Inductance analysis of the main circuit To achieve the rectification and filtering function simultaneously, we need to design the inductance of the auxiliary converter. For rectifier function, the converter should achieve unit power factor rectification. Therefore, to ensure a low harmonic component value, the inductance value should not be too small. For the filter function of the converter, it is required to produce a compensation current that is reverse to the primary harmonic current. Especially for the middle and high frequency harmonics, it is required that the compensation current can track the harmonic current instruction without error. At this time, the inductance value cannot be too large. Therefore, the two functions need to be taken into consideration in analyzing the inductance value, which is related to the change rate of harmonic current, switching frequency, current amplitude, and so on.

3.2.1. Inductance design of the rectification function Figure 7 is the equivalent circuit diagram of the auxiliary converter, u_c is the voltage of the auxiliary winding, L_3 is the equivalent inductance, C is the supporting capacitor, R is the equivalent load, and U_d is the auxiliary DC voltage. For the function of rectification, the value of inductance is shown in formula (12) [23].

$$L_3 < \frac{\sqrt{U_d^2 - U_m^2}}{I_m \omega_1} \tag{12}$$

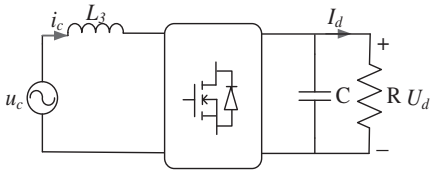

Multiple
function APU

Fig. 7. Auxiliary converter circuit

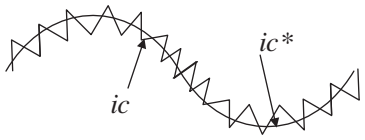

Fig. 8. Tracking principle of reference current

where U_m is the peak value of AC voltage, I_m is the peak value of AC current, $ic = I_m cos\omega t$.

At the same time, in accordance with the AC side current ripple of no more than 10% [25],

$$L_3 \geq \frac{|\ U_m \sin \omega t - sU_d\ |}{4 f_s I_m \times 10\%} \tag{13}$$

f_s is the switching frequency, s is the switching function (1/0).

3.2.2. Inductance design for tracking performance The AC side inductance current of the auxiliary winding is zigzagged along the reference current, as shown in Fig. 8.

i_c* is the reference current, i_c is the tracking current.

For this topology, the inductance current is shown as follows:

$$\frac{di_{L_3}}{dt} = \frac{1}{L_3}(u_c - sU_d) \tag{14}$$

In this formula, i_{L3} is the inductance current, u_c is the voltage of auxiliary winding, s is the switching function.

From formula (14), we can find that with the increase of L_3, the slope of the inductance current gets smaller, and the tracking performance of compensation current is poorer.

The harmonic current produced by the four quadrant converter is shown in formula (1).

To ensure that the inductor current can track the reference harmonic current, the change rate of inductance current should be greater than the change rate of the harmonic current.

$$\frac{di_{L_3}}{dt} > i'_{ch\max} \tag{15}$$

$$i'_{\mathrm{chmax}} = {i_{Nn}}'(t) \cdot \frac{n_2}{n_3} = \frac{4U_{dc2}}{m\pi L_2} J_n \left(\frac{m\pi M}{2}\right) \cos\frac{m\pi}{2} \sin\frac{n\pi}{2} \cdot \frac{n_2}{n_3} \tag{16}$$

The range of the inductor value:

$$L_3 < \frac{|u_c - sU_d|}{|i'_{ch\max}|} \tag{17}$$

According to formula (17), the range of inductance is related to the switching frequency of the traction side, it is also related to the highest harmonic frequency that needs to be suppressed. To satisfy the tracking performance of current, the larger the ${i_{chmax}}'$, the smaller the upper limit of the inductance.

Considering the current tracking performance of the filter function, rectifying function and the converter unit power factor,

and ripple characteristic of the AC side, the inductance value range is shown in formula (18).

$$\begin{cases} \frac{|U_m \sin \omega t - sU_d|}{4 f_s I_m \times 10\%} \le L_3 \le \frac{|u_c - sU_d|}{|i'_{ch\max}|} \\ L_3 \le \frac{\sqrt{U_d^2 - U_m^2}}{I_m \omega_1} \end{cases} \tag{18}$$

From formula (18), we can find that the inductance value is influenced by switching frequency, with the increase of switching frequency f_s, the limit of inductance gets lower, and the tracking performance of the reference current becomes better. The inductor value is also affected by the harmonic frequency and amplitude, as well as the current of the auxiliary side.

4. Digital Implementation of Multi-Function Converter Control Scheme

4.1. Introduction of the converter control scheme

In the proposed method, the active filter function is not always enabled. In this scheme, the compensation current is generated only when the possibility of resonance accident is identified.

For the identification method, the method mentioned in references 26, 27 is used. We define the resonance characteristic value H:

$$H = \frac{U_{pcch}}{U_{abh}} \tag{19}$$

Here, u_{abh} is the pulse voltage of the traction converter, u_{pcch} is the voltage at pantograph. If the value of H is larger than a set value, the active filter function is active to avoid resonance until the value of H is detected to be lower than the set value. The set value is designed according to the voltage by the sensors, which is related to parameters of lines and locomotives.

Figure 9 shows the control block diagram of the main circuit and multifunction converter. Fundamental current control and DC voltage control are mainly applied to achieve unity power factor rectification function. The error of reference value u_d* and measured value u_d of DC voltage is transferred to the PI controller, where the reference value of amplitude of AC side current $I_{c31}*$ is obtained, then the reference fundamental current $i_{c31}*$ is produced by multiplying the phase. The error of reference current and measured current would flow through the proportional controller to realize fast tracking of the fundamental current.

Harmonic current controller is applied to complete the filter function of the converter. The harmonic current of the primary side i_{ph} is obtained by detecting and discrete Fourier analyzing of the primary side current. The reference current is $i_{ph}* = 0$, and proportional resonance controller is applied to track the reference current with no error. Therefore, the compensation current is generated.

There are two auxiliary converters. To have a better performance on active filter function, only one auxiliary converter is used to generate the compensation current.

Block diagram of Discrete Fourier Analysis is shown as follows: In this article, sliding window Fourier transform is used.

$$i(k) = \sum_{n=1}^{N\max} \left\{ A_n \cos\left(nk\frac{2\pi}{N}\right) + B_n \sin\left(nk\frac{2\pi}{N}\right) \right\} \tag{20}$$

$$A_n = \frac{2}{N} \sum_{x=x_{new}}^{x_{new}-N+1} \mathrm{i}(x) \cos\left(nx\frac{2\pi}{N}\right)$$

$$= \frac{2}{N} \begin{Bmatrix} \sum_{x=x_{new}-1}^{x_{new}-N} \mathrm{i}(x) \cos\left(nx\frac{2\pi}{N}\right) - \mathrm{i}(x_{new} - \mathrm{N}) \\ \cos\left[n\left(x_{new} - N\right)\frac{2\pi}{N}\right] \\ + i\left(x_{new}\right) \cos\left(nx_{new}\frac{2\pi}{N}\right) \end{Bmatrix} \tag{21}$$

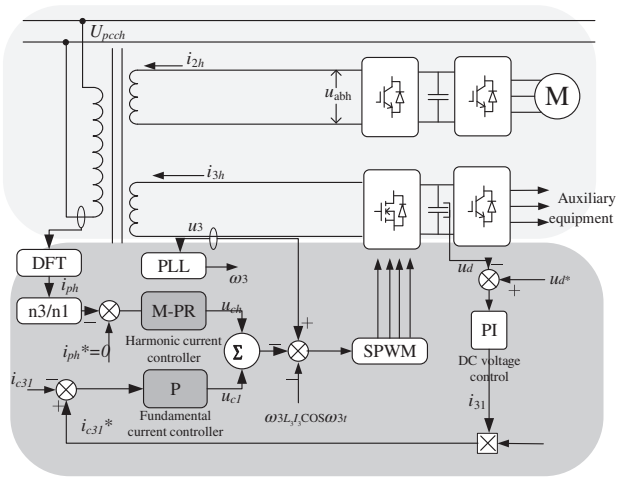

Fig. 9. Electric locomotive main circuit and control scheme block diagram

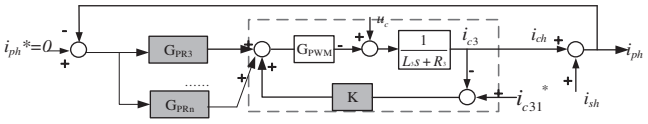

Fig. 10. Auxiliary converter current loop control block diagram

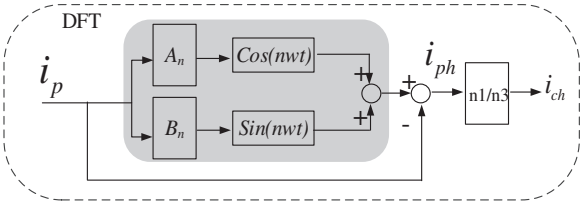

Fig. 11. Fourier analysis block diagram

$$B_n = \frac{2}{N} \sum_{x=x_{new}}^{x_{new}-N+1} \mathrm{i}(x) \sin\left(nx\frac{2\pi}{N}\right)$$

$$== \frac{2}{N} \begin{Bmatrix} \sum_{x=x_{new}-1}^{x_{new}-N} \mathrm{i}(x) \sin\left(nx\frac{2\pi}{N}\right) - \mathrm{i}(x_{new} - \mathrm{N}) \\ \sin\left[n\left(x_{new} - N\right)\frac{2\pi}{N}\right] \\ + i\left(x_{new}\right) \sin\left(nx_{new}\frac{2\pi}{N}\right) \end{Bmatrix} \tag{22}$$

In the formula (22) above, N is the window length, x_{new} is the new data point, when $n = 1$, the fundamental current is extracted, the harmonic current is obtained by primary side current minus fundamental current.

Current loop control block diagram is shown in Fig. 10, i_{c31} is the AC side current of the auxiliary converter. The error flows through the controller K to track the fundamental current, G_{PWM} is a PWM link, which is usually replaced by a first order inertia link (Fig. 11).

$i_{ph}*$ is the reference harmonic current of the primary side, whose value is zero. The input of the multiple-proportional resonance (M-PR) controller is the error of the reference value and the feedback value. M-PR is applied to produce the compensation current until the harmonic current is filtered. In formula (23), K_p is the proportional coefficient, K_{rh} is the resonance coefficient, and $h\omega_0$ is the resonance angle frequency.

$$G_{PR}(s) = K_p + \sum_{h=2,5,7,11\ldots} \frac{K_{rh} s}{s^2 + (h\omega_o)^2} \tag{23}$$

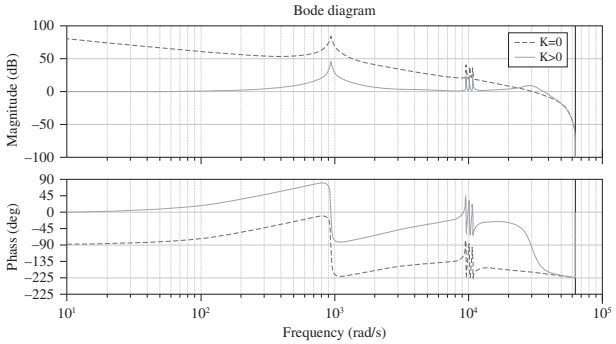

Fig. 12. The influence of feedback K on the phase margin

In practical applications, it is necessary to consider the rounding error and truncation error existing in the digital control system, where the quasi-resonant controller is used instead of the ideal PR controller.

$$GPR(s) = Kp + \sum_{h=3,31,33,35} \frac{2Krh\omega chs}{s^2 + 2\omega chs + h\omega_0^2} \tag{24}$$

When the input of the fundamental is 0, the transfer function about the input and output of the harmonic is obtained, and a feedback K is introduced at this time. Open loop transfer function of harmonic current control is shown in (25).

$$H_0(s) = G_{PR}(s)G_i(s) \tag{25}$$

where $G_i(s)$:

$$G_i(s) = G_{PWM}(s) \cdot \frac{1}{(L_s S + R)} / \left[1 + G_{PWM}(s) \cdot \frac{1}{(L_s s + R)} \cdot K\right] \tag{26}$$

The closed loop transfer function of the harmonic controller:

$$H_c(s) = \frac{H_0(s)}{1 + H_0(s)} \tag{27}$$

To achieve fast tracking control of reference currents, and complete rectification and filtering function without affecting the stability of the system, we need to design K_{rh} and other parameters for the resonant controller. The commonly used design method is to utilize the amplitude-frequency and phase-frequency characteristic curves in the continuous domain. We can design parameters at resonant frequencies to achieve higher gain at these frequencies and to satisfy the phase-angle margin. This method is simple to understand, but the results cannot be directly applied to the digital system because of the obvious error. Therefore, in this article, the stability and parameter design of the system are analyzed by using the root locus in the discrete domain.

4.2. Discretization and stability analysis of controller

Figure 9 shows the control block diagram of the main circuit and multifunction converter.

To obtain a good tracking performance at the resonant frequency, the discretized resonant controller should keep the resonant frequency from shifting and have a large gain at this point. In this article, Tustin with prewarping method is adopted. The phase lag at the resonance point is smaller and the system is stable. And the frequency does not shift with the sampling frequency after discretization. The discrete factor is:

$$s = \frac{\omega}{\tan(T/2)} \cdot \frac{z-1}{z+1} \tag{28}$$

The traditional Bode diagram of the resonant controller transfer function is shown as the dotted line in Fig. 12, here $K = 0$.

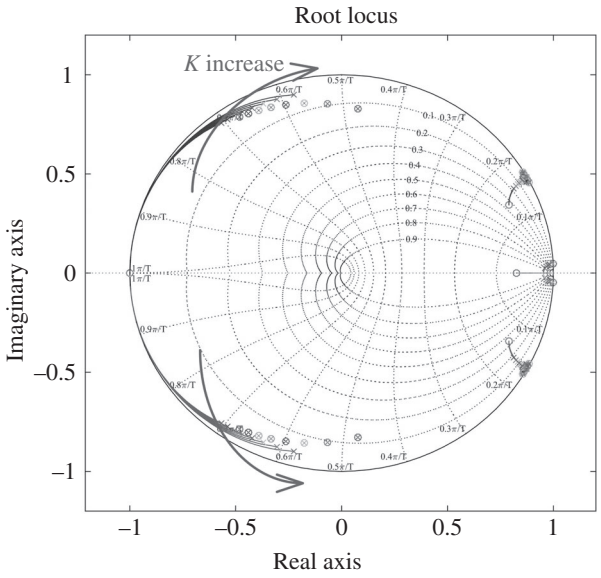

Fig. 13. Effect of K value on system stability

From the parameters provided by Toshiba China Co., Ltd., the switching frequency of traction 4QC is 450 Hz, and unipolar modulation is applied, so the equivalent switching frequency is 900 Hz, the harmonics are near the integer time of the switching frequency, for example two times of 900 Hz (1800 Hz). After investigation of a large number of accidents happened in China, the accident frequency focused on 1550, 1650, and 1750 Hz, which are around 1800 Hz, so we choose these three frequencies to analyze.

When considering the digital control delay T_{PWM} of the current loop, a pole $p = -1/(1.5T_{PWM})$ on the real axis is added to the open loop transfer function of the current loop. The pole is far from the origin and can be ignored when the harmonic frequency is low. However, as the harmonic frequency increases, the digital delay will reduce the phase margin of the current loop. The higher the frequency of the harmonic, the greater the phase lag caused by the digital delay link. Because the PR controller in the current loop has a phase jump near the resonant frequency, if it is not properly compensated, the phase angle margin of the system will continuously decrease, leading to instability of the system. With the increase of the harmonic frequency that needs to be suppressed, the phase frequency characteristics will probably pass through 180°, making the current loop unstable. Therefore, for a conventional resonant controller, when the number of suppressed harmonics is high, the delay of the current loop must be compensated. The system would be more complex.

In this article, a feedback controller is introduced into the harmonic current controller. When $K > 0$, the phase margin of the system is obviously improved, and the system can remain stable at a higher resonance frequency. When the value of the parameter K changes, the root locus of the closed loop system is shown in Fig. 13, at this time, the root trajectory is within the unit circle, which means the system can remain stable. When K increases, the root locus approaches to the border, the system is more sensitive to the disturbance. Therefore, K should be limited to the appropriate range, here the value of K is chosen as 5.

4.2.1. Effects of sampling frequency and the number of paralleled controllers When the sampling frequency is high, the system could be transformed from continuous domain to discrete domain with a better performance. However, when the sampling frequency is low, the Nyquist frequency of the control system approaches to the resonant frequency, leading to instability of the system. Figure 14 shows the root locus of the system when the sampling frequencies are 5, 10, and 20 kHz, respectively.

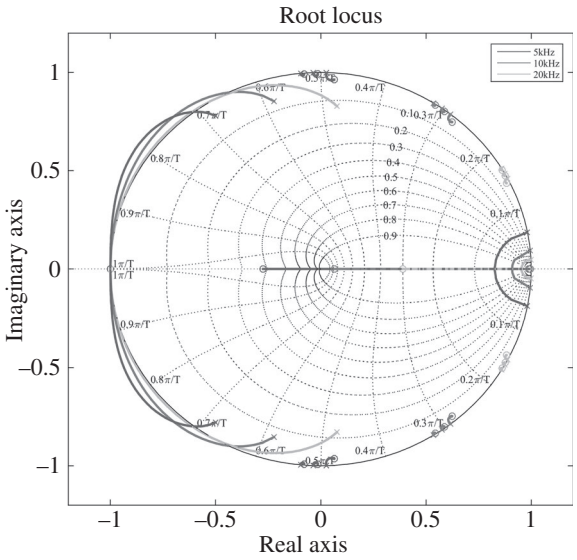

Fig. 14. Closed loop root locus when sampling frequency changes

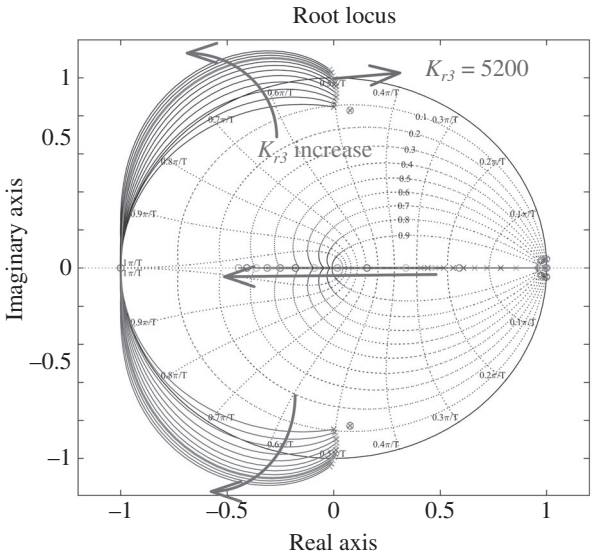

Fig. 16. Root locus when *Kr3* changes

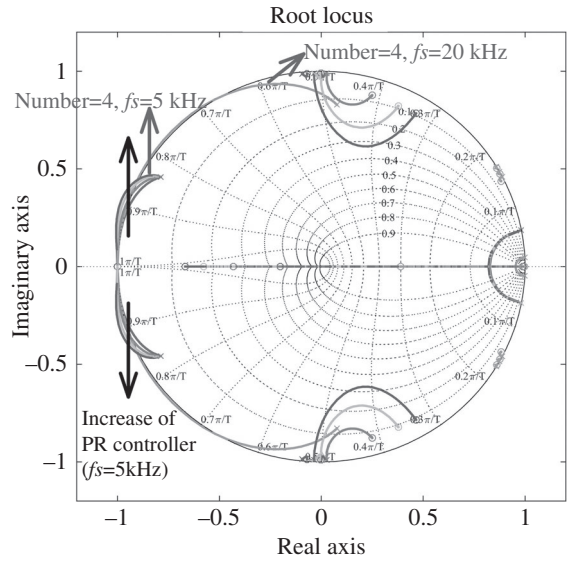

Fig. 15. Closed-loop root locus when the number of parallel resonant controllers changes

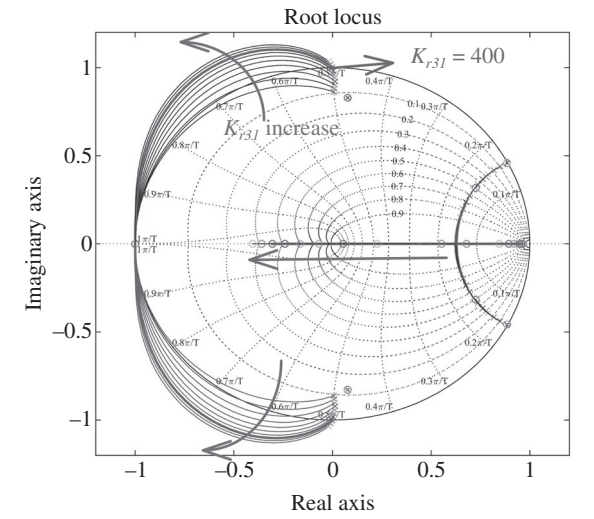

Fig. 17. Root locus when Kr31 changes

As can be seen from the diagram, with the reducing sampling frequency, the stable range of the system gets smaller.

When the sampling frequency is constant, the system tends to be unstable with the increase of the resonant controllers. As shown in Fig. 15, at a sampling frequency of 5 kHz, the root locus moves to out of the unit circle with the number of resonance controllers increasing. For the control strategy in this article, multiple resonance controllers are required. Under the condition that the sampling frequency is 20 kHz, part of the system root locus is within the unit circle. To ensure that the system is in a stable state, a higher sampling frequency should be adopted when multiple resonant controllers are connected in parallel.

4.2.2. Parametric design and its effect on stability In this article, the resonance coefficient of the resonant controller and the cut-off frequency near the resonant point are analyzed and designed by the root locus method. For the multiplied PR controller, each resonant term has a high gain only near its resonance frequency. Therefore, when the parameters are analyzed, the resonant coefficient can be set separately to find the critical value of the resonant coefficient K_r at the corresponding frequency to simplify the process. Meanwhile, the cut-off frequency ω_{ch} is reasonably designed.

Figure 16 shows the root locus of the system when the resonant frequency is 150 Hz. As K_r increases, the root locus moves to out of the unit circle, that is, the system tends to be unstable. The distance between the closed-loop zero and pole increases, so the dynamic response of the system accelerates. After designing, the critical value of K_{r3} at this frequency is 5200.

In the same way, Fig. 17 is the root locus of the system when the resonant frequency is 1550 Hz, and the critical value of K_{r31} is 400. We can obtain the critical values of $K_{r33} < 375$, $K_{r35} < 350$.

ω_{ch} is the cut-off frequency around resonance frequency, and decides the sensitiveness to the frequency offset. According to standard of 'GB/T15945-2008' in China, offset frequency of a power system is no more than 0.2 Hz, for h-order harmonic current, offset frequency $< (0.2 \times \mathrm{h})$Hz.

According to the definition of bandwidth, we get the formula:

$$\left| \frac{2K_{rh}\omega_{ch}(j\omega)}{(j\omega)^2 + 2\omega_{ch}(j\omega) + \omega_o^2} \right| = \frac{K_{rh}}{\sqrt{2}} \tag{29}$$

At this time, the bandwidth is ω_{ch}/π, so:

$$\omega ch/\pi \geq 2 \times 0.2 \times hHz \tag{30}$$

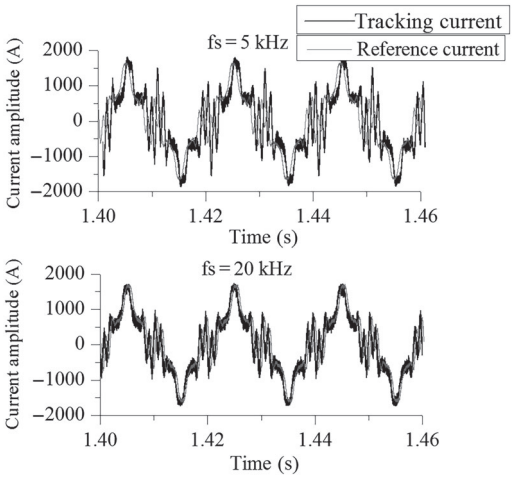

Fig. 18. Tracking performance at different switching frequencies

Table I. Main circuit parameter

Winding	Primary	Traction	Auxiliary
Rated power	7051 kVA	6400 kVA	2×217 kVA
Rated voltage	25 kV	4×1950 V	2×304 V
Rated current	282 A	4×820 A	2×714 A
DC voltage	—	3500 V	600 V
Switching frequency	—	450 Hz	20 kHz

5. Simulation and Experimental Results

This article mainly focuses on the electric locomotive, and the control strategy is verified by Matlab/Simulink. First of all, the influence of the inductance value on tracking performance is verified. Then, the feasibility of the novel control strategy of the auxiliary converter is verified by observing the power quality of the traction network.

The hardware in loop experiment is carried out by RT-LAB. The control scheme is digitalized with digital signal processor (DSP) to verify the feasibility of the control scheme for improving the power quality and restraining resonance.

5.1. Simulation verification of inductance value In Section 2.2, the inductance value is analyzed in detail. From the formula (18), the switching frequency determines the inductance value, which affects the tracking performance.

Figure 18 compares the tracking performance at different switching frequencies for the same reference current. Converter parameters are shown in Table I. The y-axis is the AC current in the auxiliary converter, the x-axis shows time.

At a frequency of 5 kHz, $L = 100\,\mu$H; When the frequency is 20 kHz, $L = 50\,\mu$H. The harmonic current frequency is around 1550 Hz. From the simulation results, we can conclude that for the same reference harmonic current, the higher the switching frequency is, the better the tracking performance of the current is, that is, the compensation current can compensate the harmonic current generated by the traction converter better. The application of *SiC* devices can increase the switching frequency and generate high-frequency compensation current while reducing the volume and losses of the converter. Therefore, this article considers the use of *SiC* devices in auxiliary converters.

5.2. Simulation verification of converter function and resonance suppression To verify the function of improving power quality in the traction network, the current is detected and analyzed by Fourier transform. Before the filter function is applied, the current spectrum of the primary side is shown in Fig. 19. Harmonic current frequencies are around 3 times of the fundamental frequency and 4 times of the switching frequency. As explained in Section 4.2, the odd harmonic values near 1800 Hz are high.

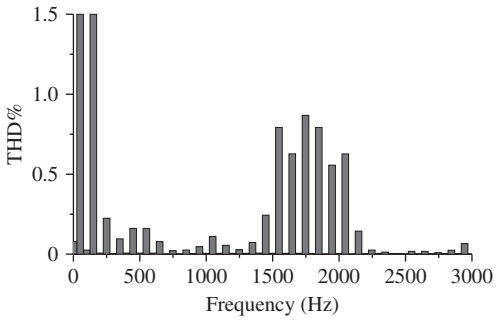

Fig. 19. Spectrum of primary side before compensation

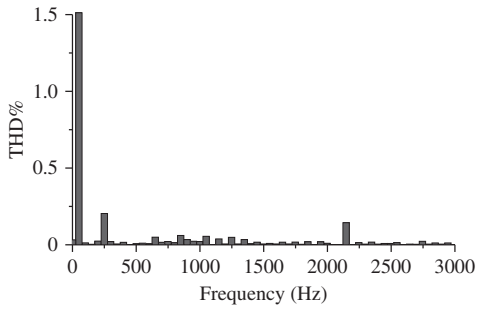

Fig. 20. Spectrum of primary side after compensation

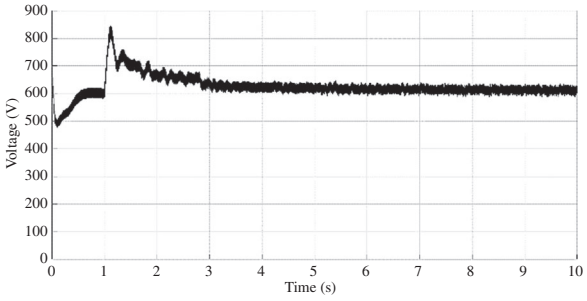

Fig. 21. DC output voltage of auxiliary converter

After the filter function is enabled, the current spectrum is shown in Fig. 20. The harmonic contents near the third harmonic and integer multiples of the switching frequency are significantly reduced, which means the harmonics generated by the traction converter could be filtered by the scheme, improving the power quality of the traction network.

Figure 21 shows the DC output voltage of the auxiliary converter. Before the filter function operates, the converter transfers the voltage of AC 304 V to DC 600 V for the inverter to supply power for auxiliary equipment. When the filtering function is started at the time of 1 s, the output voltage is disturbed and then resumes to a stable state of 600 V after the time of 2 s, which means the rectifier function of the converter can still be realized.

The T-type equivalent circuit of a certain line is established by adopting the method in Section 2.2. The impedance characteristic of the network is shown in Fig. 22. It can be seen from the diagram that the impedance of the transmission line is higher near 1550 Hz. When the certain harmonic current is injected into the line, the voltage would rise, leading to resonance accident.

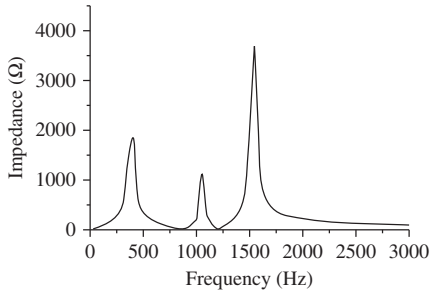

Fig. 22. Impedance characteristic of the network

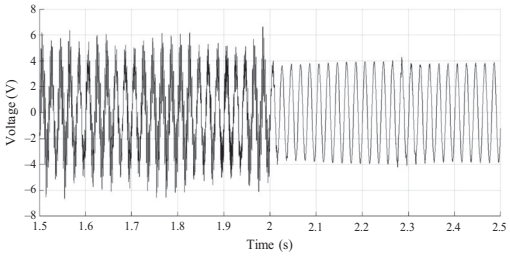

Fig. 23. Voltage of traction network

Figure 23 shows the voltage waveform of the traction network. Before the time of 2 s, the current injected by the traction converter into the traction network contains a large number of harmonics at 1550 Hz, causing resonance accident and a resonant peak voltage of over 55 kV. After the time of 2 s, the filtering function is operated, and the resonant voltage is suppressed. The peak value of the traction network voltage is $27.5\sqrt{2}$ kV, which is a normal state.

The control scheme of the vehicle converter could complete two functions of rectification and filtering, converting power for the auxiliary equipment, improving the power quality of the traction network, and suppressing the resonance voltage. Aiming at high-frequency harmonic, the *SiC* devices are applied to auxiliary converters, thereby improving switching frequency, reducing loss and weight, and meeting the trend of lightweight in rail transit.

5.3. Analysis of the experimental results To verify the feasibility of the control algorithm, the RT-LAB semi physical platform is used to carry out the experiment and digitize the control scheme.

5.3.1. Introduction of the RT-LAB platform Figure 24 shows the block diagram of the hardware in the loop experimental platform, which is composed of the computer, the OP5600 simulator, and the DSP + field-programmable gate array (FPGA) controller.

In the experiment, due to the low calculation precision of the platform, the maximum switching frequency is 5 kHz, which is much lower than the frequency of 20 kHz applied in simulation. Therefore, the harmonic to be suppressed should be lower. The rectifier function and harmonic suppression function of the converter are verified when the harmonic frequencies are 150 and 850 Hz. Another characteristic frequency of the resonance accidents is 850 Hz.

5.3.2. Experimental results of harmonic suppression When the harmonic current is 3.6 A, 150 Hz is injected into the traction network, the measured fundamental current value in the primary side is 371 A. Before filtering, the spectrum of the primary side current is shown in Fig. 25, total harmonic distortion (THD)% at 150 Hz is 1.05%.

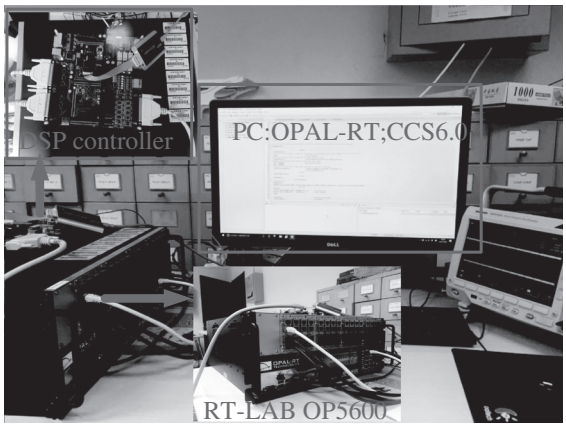

Fig. 24. RT-LAB platform

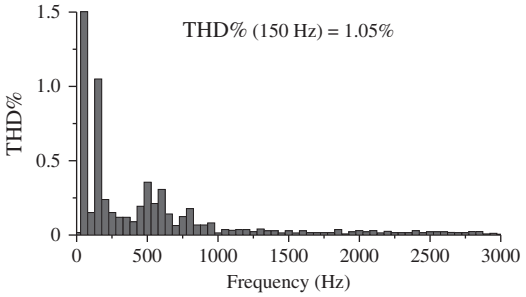

Fig. 25. Spectrum of the primary side before compensation (150 Hz)

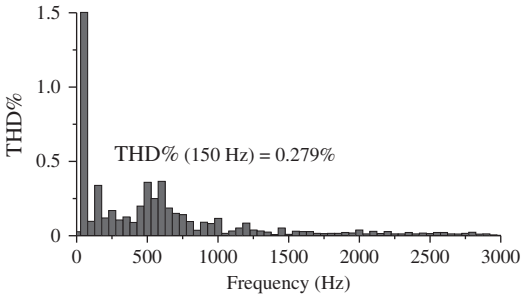

Fig. 26. Spectrum of the primary side after compensation (150 Hz)

After filtering, the THD% at 150 Hz is decreased to 0.279%.

For the 850 Hz harmonic current, THD% is decreased from 0.927 to 0.292%.

From the experimental results, we can come to the conclusion that for the harmonic current at 150 and 850 Hz, the converter can improve the power quality of the traction network.

6. Conclusion

To improve the quality of electric power injected into the traction network and to suppress the resonance voltage, the novel control scheme for auxiliary converter is proposed.

For this scheme, the main circuit inductance of the auxiliary converter is analyzed, the value is influenced by switching frequency of auxiliary converter and harmonic frequency of the traction converter. To compensate the high frequency current, the switching frequency of the auxiliary side is chosen as 20 kHz, At the same time, by applying *SiC* devices, a good suppression performance can be achieved, reducing losses, volume, and weight

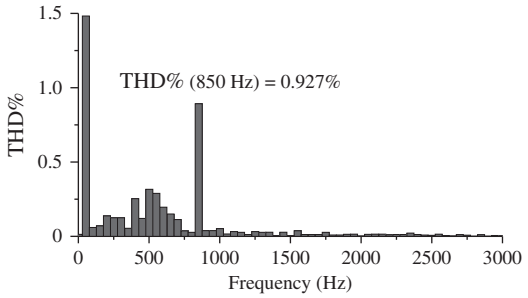

Fig. 27. Spectrum of the primary side before compensation (850 Hz)

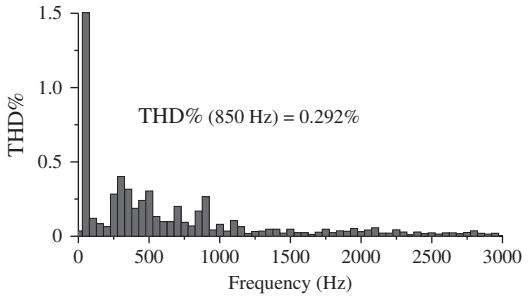

Fig. 28. Spectrum of the primary side after compensation (850 Hz)

of the converter, which is conducive to the lightweight and environmentally friendly development of rail transit.

For the purpose of putting this method into practice, the digital implementation of the control scheme is produced. Tustin with prewarping method and root locus is applied to analyze the critical value of parameters and to analyze the stability of the system. For the multiple resonance controller, the sampling frequency is 20 kHz. At the same time, the feedback control is introduced to increase the phase margin so as to obtain a stability system. By simulations and experiments, the feasibility of the control scheme of the multifunction converter is verified, the power quality of the electrified railway is improved, and the resonance accident could be suppressed.

Acknowledgments

This work was supported by the Fundamental Research Funds for the Central Universities under Grant 2018YJS158 of China. In addition, Toshiba China Co., Ltd also provided support in testing.

References

(1) Schmid F, Goodman CJ. Overview of electric railway systems. *Professional Development Course on Electric Traction Systems*, IET, 2015; 1–15.

(2) Song K, Konstantinou G, Wu M, Acuna P, Aguilera RP, Agelidis VG. Windowed SHE-PWM of interleaved four-quadrant converters for resonance suppression in traction power supply systems. *IEEE Transactions on Power Electronics* 2017; **32**(10):7870–7881.

(3) Hu H, He Z, Gao S. Passive filter design for China high-speed railway with considering harmonic resonance and characteristic harmonics. *IEEE Transactions on Power Delivery* 2015; **30**(1):505–514.

(4) Vaclav K, Bohumil S. Effect of filter and compensation unit in the traction power supply at extreme distortion. *International Conference on Compatibility and Power Electronics*, 2013; 7–12.

(5) Kwon KM, Song YS, Choi J. 6MVA single-phase APF for high speed train line in Korea. *International Conference on Power Engineering and Renewable Energy*, IEEE, 2015; 31–36.

(6) Bueno A, Aller JM, Restrepo JA, Harley R, Habetler TG. Harmonic and unbalance compensation based on direct power control for electric railway systems. *IEEE Transactions on Power Electronics* 2013; **28**(12):5823–5831.

(7) Mochinaga Y, Hisamizu Y, Takeda M, Miyashita T, Hasuike K. Static power conditioner using GTO converters for AC electric railway. *Power Conversion Conference*, Yokohama, Japan, 1993; 641–646.

(8) Uzuka T, Ikedo S, Ueda K. A static voltage fluctuation compensator for AC electric railway. *IEEE Power Electronics Society 35th Annual Power Electronics Specialists Conference*, 2004; 1869–1873.

(9) Juanlong W, Wensheng S, Xinglai G, Wenming Z, Xiaoyun F. A harmonic resonance suppression scheme for high speed railway traction power network based on single-phase LCL pulse rectifiers. *Journal of The China Railway Society* 2016; **38**(3):27–35.

(10) Maeda T, Watanabe T, Mechi A, Shiota T, Lida K. Hybrid single-phase power active filter for high order harmonics compensation in converter-fed high speed trains. *Power Conversion Conference - Nagaoka 1997*, vol. 2, 2002; 711–717.

(11) Sato K, Kato H, Fukushima T. Development of SiC Applied Traction System for Shinkansen High-speed Train. *International Power Electronics Conference*, 2018; 3478–3483.

(12) Li H, Zhang K, Zhao H, Fan S, Xiong J. Active power decoupling for high-power single-phase PWM rectifiers. *IEEE Transactions on Power Electronics* 2013; **28**(3):1308–1319.

(13) Basic D, Ramsden VS, Muttik PK. Harmonic filtering of highpower 12-pulse rectifier loads with a selective hybrid filter system. *IEEE Transactions on Industrial Electronics* 2001; **48**(6):1118–1127.

(14) Loh PC, Yang Y, Blaabjerg F, Wang P. Mixed-frame and stationary-frame repetitive control schemes for compensating typical load and grid harmonics. *IET Power Electronics* 2011; **4**:218–226.

(15) Herman L, Papic I, Blazic B. A proportional-resonant current controller for selective harmonic compensation in a hybrid active power filter. *IEEE Transactions on Power Delivery* 2014; **29**(5):2055–2065.

(16) Liserre M, Teodorescu R, Blaabjerg F. Multiple harmonics control for three-phase grid converter systems with the use of PI-RES current controller in a rotating frame. *IEEE Transactions on Power Electronics* 2006; **21**(3):836–841.

(17) Asiminoaei L Blaabjerg F, Hansen S. Evaluation of harmonic detection methods for active power filter applications. *Power Electronics Conference and Exposition*, 2005; 1 635–641.

(18) Yepes AG, Freijedo FD, Doval-Gandoy J, López Ó, Malvar J, Fernandez-Comesaña P. Effects of discretization methods on the performance of resonant controllers. *IEEE Transactions on Power Electronics* 2010; **25**(7):1692–1712.

(19) Luo A, Chen Y, Shuai Z, Tu C. An improved reactive current detection and power control method for single-phase photovoltaic grid-connected DG system. *IEEE Transactions on Energy Conversion* 2013; **28**(4):823–831.

(20) Yang H, Lin H, Lv Y, Luo Y, Wang X. A multi-resonant PR inner current controller design for reversible PWM rectifier. *Applied Power Electronics Conference and Exposition, IEEE*, 2013; 316–320.

(21) Lascu C, Asiminoaei L, Boldea I, Blaabjerg F. High performance current controller for selective harmonic compensation in active power filters. *IEEE Transactions on Power Electronics* 2007; **22**(5):1826–1835.

(22) Wang J, Trillion QZ, Gao J, Jianqiang L. Design of current regulator for single-phase PWM rectifier with low switching frequency based on bode diagram. *International Conference on Electrical Machines & Systems*, 2011; 1–1.

(23) Sheng CF , Liu YJ, Lin F, You XJ, Zheng TQ. Power quality analysis of traction supply systems with high speed train. *IEEE Conference on Industrial Electronics & Applications*, 2009; 2252–2256.

(24) Chu X, Lin F, Yang Z. The analysis of time-varying resonances in the power supply line of high speed trains. *Power Electronics Conference*, 2014; 1322–1327.

(25) Qiang YQY , Hengbin CHC , Xinwei DXD, Wu G. A Novel Design Method of AC Side Inductance of Four-Quadrant Converter. *Power & Energy Engineering Conference*, IEEE, 2010; 1–5.

(26) Holtz J, Krah JO. On-line identification of the resonance conditions in the overhead supply line of electric railways. *Archiv fur Elektrotechnik* 1990;74(1):99–106.

(27) Holtz J, Krah JO. Suppression of time-varying resonances in the power supply line of AC locomotives by inverter control. *IEEE Transactions on Industrial Electronics* 1992;39(3):223–229.

Meijun Mu (Non-member) received her B.S. degree in electrical engineering from Beijing Jiaotong University, Beijing, China in 2016. She is currently pursuing her Master's degree in electrical engineering at Beijing Jiaotong University. Her research interests are power electronics and electrical drives.

Zhongping Yang (Non-member) received his B.Eng. degree from Tokyo University of Mercantile Marine, Tokyo, Japan in 1997, and received his M.Eng. degree and Ph.D. degree from the University of Tokyo, Tokyo, Japan in 1999 and 2002, respectively, all in electrical engineering. He is currently a Professor with the School of Electrical Engineering, Beijing Jiaotong University, Beijing, China. His research interests include high-speed rail integration technology, traction & regenerative braking technology, and wireless power transfer of urban rail vehicles. Prof. Yang received the Zhan Tianyou Award for Science and Technology in 2010, the Excellent Popular Science and Technology Book Award in 2011, and the Science and Technology Progress Award (second prize) of Ministry of Education in China in 2016.

Fei Lin (Non-member) received his B.S. degree from Xi'an Jiaotong University, Xi'an, China, M.S. degree from Shandong University, Jinan, China, and Ph.D. degree from Tsinghua University, Beijing, China, in 1997, 2000, 2004, respectively, all in electrical engineering. He is currently a Professor with the School of Electrical Engineering, Beijing Jiaotong University, Beijing, China. His research interests include traction converter and motor drives, energy management for railway systems, and digital control of power-electronic-based devices.

Shihui Liu (Non-member) received her B.S. degree in electrical engineering from Beijing Jiaotong University, Beijing, China in 2014. She is currently working toward her Ph.D degree at the School of Electrical Engineering, Beijing Jiaotong University. Her current research interests are in the areas of electric traction systems for rail vehicles, vehicle-power supply network coupling system, and power quality.